

## Color heterogeneity of building surfaces: lean image processing approach for visible reflectance characterization performance

Juan D. Blanco Cadena<sup>1</sup>, Alberto Speroni<sup>1</sup>, Andrea G. Mainini<sup>1</sup>, Tiziana Poli<sup>1</sup>

<sup>1</sup>Politecnico di Milano, ABC Department, Milan, Italy

### Abstract

Daylighting availability and uniformity depend on the interior surface reflectance ( $\rho$ ). Currently,  $\rho$  is obtained through suggested reference values (Illuminating Engineering Society 2012; CIBSE 2015; CIBSE/SLL 2011; CIBSE/SLL 2005), laboratory tests (ASTM E 903 (2012) describes a standardized procedure requiring a calibrated instrument and an as-built surface sample), or by on-site measures (based on luminance and illuminance differences). Novel methodologies compute it by integrating image processing and/or photometry, applied on false colour or HDR images. A simple procedure is needed for accurately assess, even in preliminary design phases, the reflectance of heterogeneous surface areas for new and historical buildings. In fact, heterogeneous surfaces (colour, texture, composition, ageing) difficult the accurate estimation of a representative reflectance value ( $\bar{\rho}$ ) for building simulation, leading to daylighting performance deviation. This work presents a methodology, based on a per-pixel colour reflectivity ( $\rho_{col}$ ) evaluation, to easily acquire an approximate value of the surface visible reflectance ( $\bar{\rho}_{vis}$ ). This approach gives a more global  $\bar{\rho}_{vis}$  of all surface components, aiming to improve the accuracy of the modelled daylighting analysis. Additionally, the procedure is experimented over a sample reference test room.

### Introduction

Buildings in real case scenario perform differently compared to their design. A significant gap has been identified by collecting and comparing post-occupancy and design phase performance data (De Wilde, 2014). Part of this deviation has been attributed to: occupant behavior, rooms layout (Reinhart, 2002; Wolisz, Kull, Streblow, & Müller, 2015), simulation type and robust approximations on material reflectance properties (Bremilla, Hopfe, & Mardaljevic, 2018).

Indoor daylighting depends significantly on how the incoming light is being redistributed all over the room, and it can be enhanced by different strategies both external (e.g. shading or light redirecting devices) and internal (e.g. controlling reflective surfaces). Warrier & Raphael, (2017) tested on a scaled model the use of a horizontal light shelf, which coupled with a high reflectance ceiling ( $\rho = 0.85$ ) could lead to an average illuminance level increase of 21%. Given that internal surfaces reflectance governs the dispersion of light,

suitable internal strategies guarantee the success of those applied externally. For instance (Reinhart, 2002) reported that even having a lower window height, but increasing the ceiling reflectance, electric lighting energy savings can reach up to 40%. In addition to daylighting availability,  $\rho$  can alter the circadian clock, in Cai et al. (2018) a  $\bar{\rho} = 0.8$  for all internal opaque surfaces allows to achieve sufficient circadian stimulus, even with 30% Window to Wall Ratio (WWR), on December 21<sup>st</sup>, under an overcast sky, in a perimeter room in Helsinki.

Daylighting analysis results have shown that its performance metrics are sensible to the variance of  $\rho$ , they can be determinant for achieving the design regulation requirements imposed to the building. In fact, Bremilla et al. (2018) carried out a sensitivity analysis (SA) of daylighting performance metrics, that under the Morris method, showed that with a 25% WWR and constant window visible transmittance ( $\tau_{vis}$ ) = 0.8, wall reflectance's can account for  $\frac{1}{4}$  of the variations on Total Annual Illumination (TAI) (equivalent to Annual Light Exposure (ALE)); the contribution of internal  $\bar{\rho}_{vis}$  was found to be more critical for lower WWR. In the same way, it modify the results obtained for Useful Daylight Illuminance (UDI). Mardaljevic, Bremilla, & Drosou, (2015) recalls an example in which a standard office room, with  $\tau_{vis} = 0.76$ , would require a  $\rho = 0.8$  and 0.6, for ceiling and walls respectively, to comply with the UDI<sub>100-3000</sub> >82%, whereas the values suggested by guidelines ( $\rho = 0.7$  and 0.5) would achieve a UDI<sub>100-3000</sub> = 79.7%; however, if the UDI<sub>300-3000</sub> would be applied the absolute value of the metric could vary from 45.4% to 38.7%. Samant and Yang simulated the effect of different reflectance pattern on daylighting in a case study of an atrium. This pattern hypothesis simulates differences in material reflectance for coplanar surfaces having consequences on Daylight factor (DF) distributions values.

Therefore, a more prudent procedure for selecting, estimating or computing an accurate value of  $\bar{\rho}_{vis}$  to be inserted in the simulations should be drawn to diminish the gap between real and modelled building performance. Some work has been already done to achieve this goal based on the principle applied by Wienold & Christoffersen (2006) for the evaluation of the Daylight Glare Probability (DGP) using CCD cameras; one of them is Mardaljevic et al. (2015), which conducted few test based on image processing and photometry applied on High Dynamic Range (HDR) images dealing with the

luminance and illuminance contained in their metadata. However, results still deviate largely on real cases as the performed calculation of  $\rho$  relies on the principle of diffuse reflectivity, and the specular component contribution has not been considered yet, as stated by the author.

Surfaces can be considered heterogeneous by their composition, as mosaics which are constructed according to the desired visual effect, but also to their buildability. Marbles and granites retain considerable portions of different color veins or grains. These surface types make the traditional approach described by ASTM E 903 (2012) and BSI 8493 (2010) of an area-weighted average largely time-consuming, hence unpractical or unfeasible approach to determine reflectance. Thus, a methodology similar to Mardaljevic et al. (2015), but with a different approach, is hereby presented, in which the  $\rho_{col}$  is calculated for each pixel within a flat image, containing a sample with known  $\rho$ , and the whole image colour reflectivity is calibrated with the average of the pixels constructing the reference sample with known reflectivity. Additionally, a case of daylighting performance analysis was performed to determine the possible variance.

## Methodology

The workflow of the study allows verification of required and useful data for the research work, it also permits to determine the proper settings with which the pictures should be taken and calculated. The methodology involved 7 samples to complete this portion of the study.

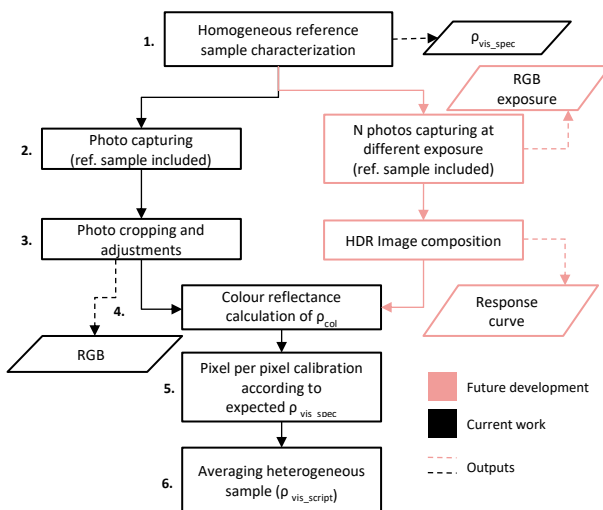


Figure 1 - Procedure schema for calculating  $\rho^*_{col}$ . The black coloured path refers to the method proposed in this paper while the pink one shows the hypothesized future approach. The dotted line shows the outputs.

The whole study can be divided into 6 parts, and a schema on how the proposed methodology is laid out is represented in Figure 1. It has extracted valuable insights from the methodology and results presented by Mardaljevic et al. (2015) however, the proposed workflow does not require explicitly HDR images; instead of 7, only 1 known reference reflectance sample

is used; and instead of punctual references, all reference sample area is used.

To understand the impact of the present work, a preliminary simulation with a reference room has been carried out.

## Sample classification, optical measurement and photograph capturing

The selected samples (see Figure 2) can be classified into three different categories:

1. Homogeneous samples (Sample A1, Sample A2, Sample A3);
2. “Small scale” heterogeneity samples (Sample B1, Sample B2, Sample B3): samples with micro differences in pigments’ colour that compose the material;
3. “Large scale” heterogeneity sample (Sample C1): sample with macroscopic differences in colouring areas.

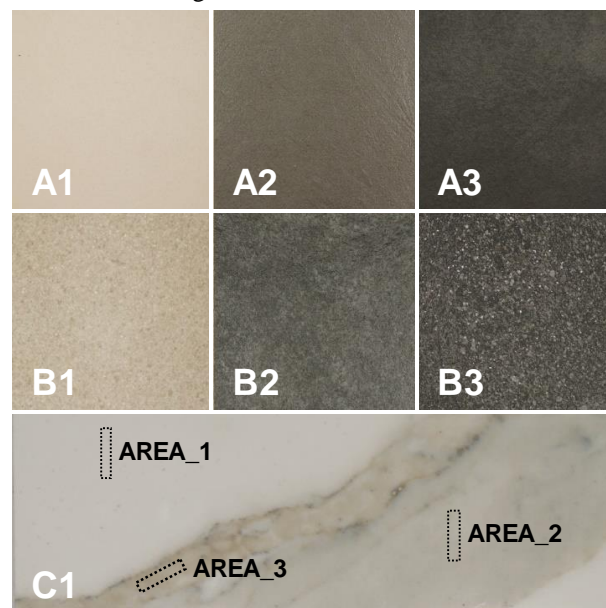


Figure 2 - Measured samples: homogeneous samples (A1, A2, A3); “Small scale” heterogeneity samples (B1, B2, B3); “Large scale” heterogeneity sample (C1). For sample C1 is also identify the 3 measurement areas: Area\_1, Area\_2 and Area\_3.

The optical characterization of the solar reflectance ( $\rho_{vis\_spec}$ ) for the selected samples has been done using the spectrophotometer Perkin Elmer LAMBDA™ 950 equipped with a 15 cm integrating sphere coated by Spectralon® that allows to measure the total reflectance from 250 to 2500 nm (entire solar spectra) with a 2 x 0,6 cm beam size in the visible spectra (ASTM international, 2012; International Organization for Standardization, 2003).

Each sample was measured in 3 spots to verify its homogeneity. For “Homogeneous” and “Small scale” heterogeneity samples the measured areas were randomly selected over the surface, while for the “Large scale” heterogeneity sample (Sample C1) the three measured

areas were previously identified and are presented in Figure 2 (Area\_1, Area\_2 and Area\_3).

The measured samples were photographed in order to calibrate the image processing script that will be explained in the following sections. The photos have been done with a Sony Alpha 6300 equipped with a lens E PZ 16-50 mm F3.5-5.6 OSS. All the photos were done with 35mm lens-length with exposure value set to zero.

### Per-pixel reflectance calculation

A script was written on the multi-propose programming language Python, using the built functions inside the OpenCV library. Assuming that  $\rho_{col} \propto \rho_{vis}$ , the script reads the RGB data of each pixel from the camera and computes  $\rho_{col}$  for each pixel following equation (1), extracted from AGi32 and ElumTools™ documentation. This equation is in accordance to the eye sensitivity to the 3 primary colours used in the most common digital colorspace (RGB), that is ~21% for Red, ~72% for Green and ~7% for Blue.

If the calculation requires calibration from a reference sample (this has been introduced to assess the variation on the surface lighting exposure when the picture is taken), then the script allows the user to navigate through the image to create a rectangular boundary around the reference sample. The average value for this sample ( $\bar{\rho}_{col\_ref}$ ) would be compared with the expected  $\rho_{vis\_spec}$ , and a correcting factor is calculated as  $k = \rho_{vis\_spec} / \bar{\rho}_{col\_ref}$  and used at each pixel. Then, extracting the pixels of the reference sample, a corrected  $\bar{\rho}_{col}$  is obtained for the desired region.

$$\rho_{col} = 0.2125 \left( \frac{R}{255} \right) + 0.7154 \left( \frac{B}{255} \right) + 0.0721 \left( \frac{G}{255} \right) \quad (1)$$

### Colour reflectance formula validation and calibration

With the values obtained from the measurements done with the standard procedure and the initial trials of the script, it was possible to evaluate the accuracy of the calculation and test its reliability. Initially, with no calibration, the  $\bar{\rho}_{col}$  was obtained for 6 homogeneous tile samples; then, formula (1) was adjusted doing a linearization of the results encountered, and then  $\rho^*_{col}$  was proposed in formula (2).

In addition, a comparison between the area-weighted approach for obtaining the mean value of a heterogeneous surface (ASTM International, 2012; British Standard Institution (BSI), 2010) and the use of the script was compared. Assuming a 2x3 grid mosaic, with the same sample distribution of samples A's and B's in Figure 2, and using each one of them as reference reflectance sample, the mean value for the hypothetic mosaic, composed by the other 5 samples, was computed.

Moreover, using the color database contained in BS 8493 and 4800 (2010, 2011), colorimetric values under CIE standard Illuminant D<sub>65</sub> (British Standard Institution (BSI), 2011b) were converted to RGB and their reflectance was computed to test the reliability of the methodology.

### $\bar{\rho}_{vis}$ estimation for a heterogeneous floor

After verifying the reliability of the calculation procedure, the methodology was applied for a heterogenous surface of an office room floor located in Milan, Italy. The photos were taken and edited following the procedure already described.

The reference sample was placed at different locations in the picture to evaluate the relevance of the edge problem effect for the calculation procedure. The value obtained was then used for the daylighting performance simulations.

### Daylighting performance simulation

The simulations were based on the model presented in Figure 3. It is a 6x8x2,7 h m room, South oriented, with two windows (3x2 m with 0,5 m height parapet) located in Milan (IWEC – weather file). The calculation grid was 0.8 m far from the floor and has a 0,3x0,3 m node density. The visual transmittance ( $\tau_{glass}$ ) of the glass is 0.86. No shading system has been considered.

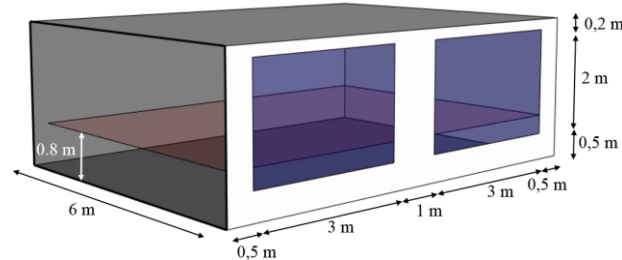


Figure 3 – Simulation model.

Most opaque building surfaces for interiors are modeled in Radiance using the primitive Plastic, which represents a type of material with a purely diffuse reflectance and which, as it is defined in Ward, G. and Shakespeare (1998). All the values are expressed in a scale between 0 and 1. In general, if the optical properties are not known, the designer has to choose among suggested values (British Standard Institution (BSI), 1985, 2008; European committee for standardization, 2011)

The reflectance values assumed in the model were:  $\rho_{wall} = 0.5$ ,  $\rho_{ceiling} = 0.8$ . The reflectance values ( $\rho_{floor}$ ) assumed for the floor were: 0.3, 0.5 and the value obtained with the proposed image processing technique.

Specularity value is used to consider the increase in specular reflection of the material and generally, a value of 0.07 is suggested, while values greater than 0.1 are generally excluded. On the other hand values over 0.2 for roughness are generally not considered.

A sensitivity analysis was performed for the same archetype of indoor environment with the aim of understanding how the arbitrary choice of floor surface specularity and roughness values, as defined in Ward, G. and Shakespeare (1998), can modify the natural light conditions inside the room.

The intensity of the variations resulting from a change in the variable surface roughness for the type of floor finishing chosen, was not evaluated parametrically. It was

therefore considered smooth, maintaining the value of roughness constant and equal to 0.02 in each of the cases represented. The specularity value was instead evaluated for three different conditions and respectively equal to 0, 0.1 and 0.2.

## Experimental Results and discussion

In summary, a total of 8 samples were assessed, and the value of  $\bar{\rho}_{vis}$  was estimated for a heterogeneous pavement, which is mainly constituted by cement screed and quarry tiles on an irregular mosaic.

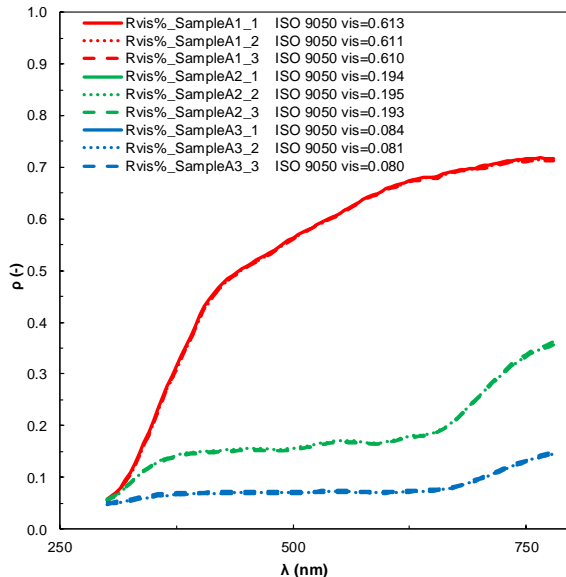


Figure 4 – $\rho_{vis}$  for samples A1, A2 and A3. The graphic shows the three measures carried out for each sample (1, 2, 3).

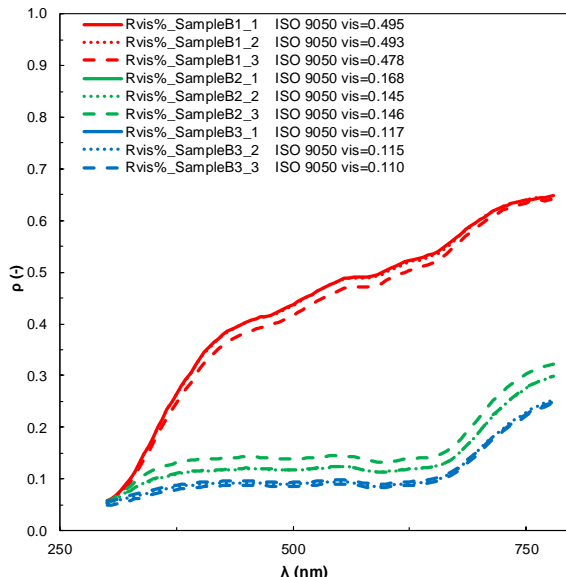


Figure 5 – $\rho_{vis}$  for samples B1, B2 and B3. The graphic shows the three measures carried out for each sample (1, 2, 3).

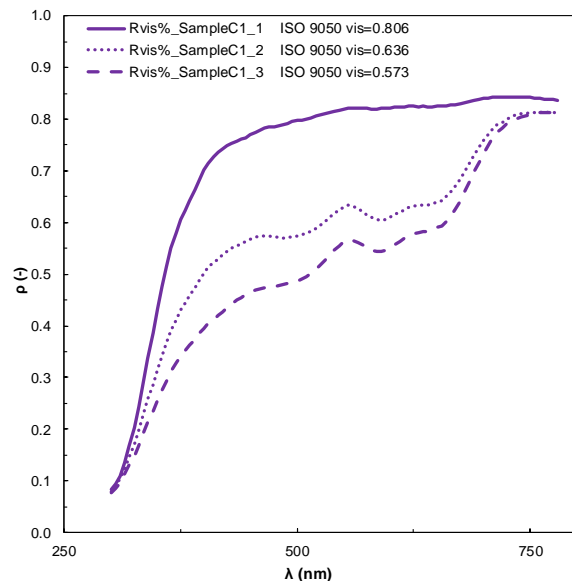


Figure 6 – $\rho_{vis}$  for sample C1. The graphic shows the three measures carried out for each sample (1, 2, 3).

### Sample characterization

The results obtained with the samples measurements are shown in Figure 4, Figure 5 and Figure 6.

The homogeneous samples (A1, A2 and A3) present very similar values for all the three measurements, as shown in Figure 4.

The “Small scale” heterogeneity samples (B1, B2 and B3) show a slight difference in the visible reflectance values for the three measurements, maintaining the same behavior of its characteristic reflectance curve because of their heterogeneity (Figure 5).

Whereas, the “large scale” heterogeneity sample (C1) shows significant differences both in the shape of the reflectance characteristic curve and in its integrated values as shown in Figure 6.

### Per-pixel reflectance calculation and calibration

From the edited pictures taken of the 6 samples, their  $\bar{\rho}_{col}$  was estimated and compared with the result obtained from the standardized characterization procedure. Even using large images (6000 x 4000 pixels), the calculation per pixel did not take more than 40 seconds per image, which already becomes an advantage compared to traditional methodologies. The graph showing the linear correlation, and the one that was used for the adjustment of  $\rho_{col}$ , is presented in Figure 7. This enabled equation (2) and the calculation of a more accurate reflectance value underline a good correlation with  $R^2 > 0.99$ .

$$\rho_{col}^* = 1.0467 \rho_{col} - 0.2267 \quad (2)$$

The algebraic differences between the initial  $\rho_{col}$  values and the  $\rho_{vis\_spec}$  for each of the previous calculations ranged between 0.169 and 0.226, having a worse estimation of the dark samples. This deviation can be attributed to the lighting conditions when the picture was taken, the camera itself and/or any specular component of the reflectance (alters the result as stated by Mardaljevic

et al. (2015)). The lighting exposure issue is expected to be corrected from the calibration, when a reference sample is used within the image captured. Regarding the variance related to the camera, it will be assessed by composing HDR and correcting the colour assigned to the pixel using the camera response curve, which has been foreseen as a future work (see Figure 1).

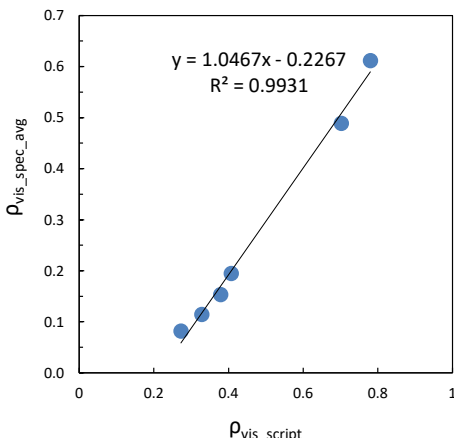


Figure 7: Equation calibration, instrument measurement vs script results.

#### • Trials on homogeneous samples

Using equation 2 the values fit more, obtaining a minimum algebraic difference of 0.007 for the Sample\_B3, and a maximum of 0.023 for Sample\_A3. Then, an additional test was carried out, targeting the Light Reflectance Value (LRV) reported for 10 color codes, using their colorimetric values (X,Y,Z of the CIE color space) under CIE standard Illuminant D<sub>65</sub> (British Standard Institution (BSI), 2010), the results can be considered satisfactory as the maximum absolute algebraic difference was 0.11, and still no further correction has been applied to the equation.

#### • Trials on heterogeneous surfaces

Also, the script was tested to verify how it would perform on a heterogeneous sample (C1) which, as seen on Figure 2, has some portions with a significant difference in  $\rho_{vis}$ . This feature can lower the average value, depending on the amount of measures that the technician will perform, and the location in which they will be done. The irregular shape of these portion impedes a proper determination of the area it covers, hence increasing the uncertainty of  $\bar{\rho}_{vis}$ . From the measurements, Sample\_C1 records a  $\bar{\rho}_{vis\_spec\_avg} = 0.672$  (performing 3 different measurements, one per each different section), and the script would recommend a  $\bar{\rho}^*_{vis\_script} = 0.504$  which could modify greatly the daylighting performance of a building with an ~0.17 difference in interior surfaces' reflectance.

#### • Lighting correction trials, with relative measurement

The grid test was performed to see how good the script was able to weight the reflectance values across the images to evaluate an overall  $\bar{\rho}_{vis}$  from a boundary, surrounding a sample with known  $\rho_{vis\_spec}$ , and compared to the area-weighted procedure normally applied. The results have been summarized on Table 1, showing that

the script is performing well (minimum absolute algebraic difference was 0.01 and the maximum was 0.107).

Apart from Sample\_A3 and Sample\_B2 (differences >0.03), most of the samples show a slight difference ~0.01. For Sample\_B2 its odd response can be attributed to the fact that it is not entirely homogeneous (brighter dots, are not evenly distributed around it).

Table 1: Grid relative measure trial.

Reference Sample	Mosaic reflectance			
	Sample	$\rho_{vis\_spec}$	$\rho_{vis\_avg}$	$\rho^*_{vis\_script}$
Sample_A1	0.611	0.206	0.221	0.015
Sample_A2	0.194	0.290	0.278	0.012
Sample_A3	0.081	0.312	0.419	0.107
Sample_B1	0.153	0.298	0.263	0.035
Sample_B2	0.489	0.231	0.220	0.011
Sample_B3	0.114	0.306	0.292	0.014

Before testing the script with the heterogeneous floor surface, a proper reference sample had to be selected. From the results presented in Table 1, Sample\_A3 had already been discarded because of its large surface reflectance deviation, followed by Sample\_B1 and Sample\_B3 which are only seemingly homogeneous, and their pattern could change the final output. In addition, Sample\_A2 presents a slight roughness that could modify the results due to angularity and Sample\_B3 seem to have embedded small crystals that could alter the outcome. Finally, Sample\_A1 seems like a more suitable reference sample to go on with the methodology reliability analysis, being homogeneous, flat and having a smooth surface. This sample is to be considered as representative for this evaluation procedure. Future versions of the project workflow will use a unique sample that, thanks to its characteristics of universality, can be reproduced by anyone who wishes to make similar studies.

A sensitivity analysis was carried out to establish the possible implications that specularity could have on the results of the daylight simulation analysis and to assure that the results later presented are consistent, if neglected.

#### • $\bar{\rho}_{vis}$ for a heterogeneous floor in an office space

The selected reference sample, was placed on top of the pavement, in the centre of the scene, of the images that were produced with the camera. This location was preferred to avoid problems dealing with photograph distortion that might occur at the edges. The results are shown in Figure 8, displaying a density frequency of the  $\rho_{col}$  of each pixel, and a heatmap that gives a better impression on how these values are distributed along the area. The density distribution (Figure 8a) presents values for  $\rho_{col} = 0$ , as they correspond to the space from which the reference sample area was extracted; also, it records values  $\rho_{col} < 0$ , which are a consequence of the adjustment in equation (2) which contribute to a more accurate  $\bar{\rho}_{col}$ . The value obtained for  $\bar{\rho}_{vis}$  was 0.42 and it was used for comparison with the suggested values found in design guidelines.

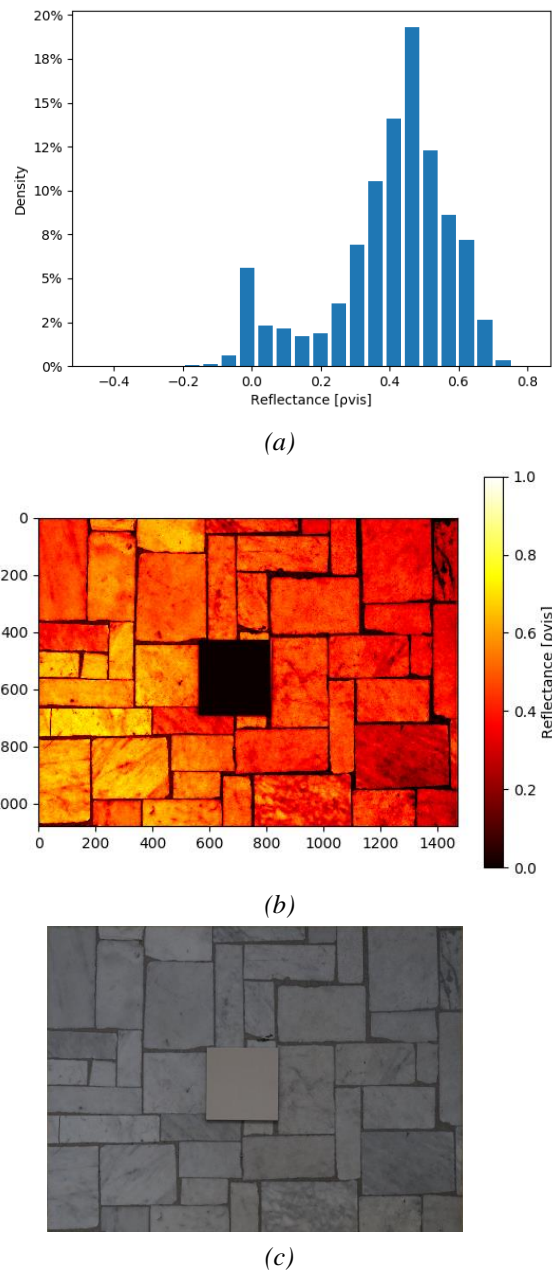


Figure 8: Pavement analysis with the proposed methodology. (a) Color reflectance frequency density; (b) Colour reflectance heat map; (c) Original picture.

#### Daylighting performance evaluation

The daylighting simulations performed are based on the model previously described. These were run to understand to what extent a simplified assumption can affect the final outcome. For this reason, three parameters were analysed: Useful daylight illuminance (UDI), Continuous Daylight Autonomy (CDA) and Daylight Autonomy (DA).

Table 2 – UDI, CDA and DA for the assumed simulation model located in Milan with south orientation.

	UDI (100-2000)	CDA	DA
$\rho_{floor}=0.3$	52.77 %	91.4 %	86.39 %
$\rho_{floor}=0.43$	48.56 %	91.94 %	87.39 %
$\rho_{floor} = 0.5$	46.33 %	92.17 %	87.89 %

The results presented in Table 2 shows that the assumption of lower  $\rho_{floor}$  values (0.3 in this study case), compared to the real one (0.43 in this study case), determined as a consequence higher UDI values (+8%) and lower values of CDA (-0.5%) and DA (-1.1%). On the other hand, the assumption of higher  $\rho_{floor}$  values (0.5 in this study case), compared to the real one (0.43 in this study case), had as a consequence lower UDI values (-4.6) and higher of CDA (+0.3%) and DA (+0.6%) values.

The results here presented can be also affected by other environmental variables and features of the model itself (i.e. room shape, location, orientation and materials).

#### Specularity sensitivity analysis of daylighting simulations

Illuminance values over the workplane for Milan IWEC weather conditions and during 21 Dec and 21 Jun at 12:00 where compared with different floor surfaces settings.

Even if a specularity value higher than 0.1 is not normally considered as realistic and representative of the type of material selected, the same value has been reported to compare the relationship between the variation of the variable and the obtainable result, as well as the effect that could be generated using these values by a non-expert user.

The main comments address the results due to a change of the specularity value between its minimum, equal to 0 and the maximum equivalent, according to Radiance reference manual (Ward, G. and Shakespeare, 1998), equal to 0.1. In general, the increase in specularity generated an increase in minimum, maximum and average illuminance values measured on the analysis grid. The illuminance values frequency distributions over the work plan presented in Figure 9a,b clearly describe the effect of light distribution inside the room. In accordance with the specularity increase, the frequency distribution had a peak shift towards higher values of illuminance and a general redistribution that could be comparable to an increase in surface reflectance instead of the sole specularity.

The absolute minimum gained the largest increase and was equivalent to about 7-10% depending on the considered day of the year (21 Dec or 21 Jun). The absolute maximum, on the other hand, showed negligible variations. Different considerations could have been made for the average indoor illuminance value.

The greatest percentage increase, due to specularity change, occurred in the period in which is normal to have a strong difference between the maximum and the average illuminance value recorded over the work plane. This happened every time higher solar altitude occurred in contemporary with greater natural light availability, generating a peak in direct natural light availability mainly in correspondence of the small grid portion facing the window surface (21 Jun - Figure 9b).

With the same reflectance of the room surfaces, the increase in floor specularity allowed an improved penetration and distribution of solar radiation in the direction of the depth of the room, increasing the absolute

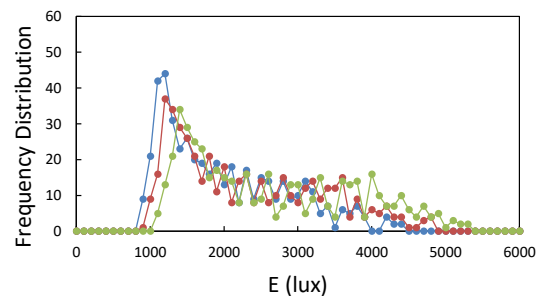
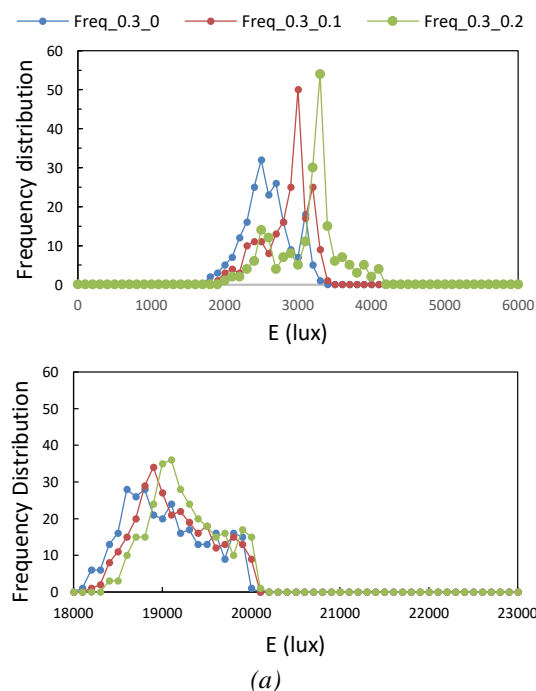
value of the average distribution. On the contrary, during the winter period (21 Dic) there was a strong non-homogeneity in the light distribution because large portions of the work plane were invested by direct light (Figure 9b). In this case, the reduced solar height allowed direct solar radiation to penetrate deeply into the room, crossing its entire depth.

Due to higher average illuminance values over the visual task area, the effectiveness of specularity change was less significative (more than 1%).

Table 3: Change in illuminance values over the work plane due to a change in floor specularity.

Specularity	E [lux]			$\Delta\% [\%]$		
	0	0.1	0.2	0	0.1	0.2
21-Jun	min	820	899	1019	-	9.6% 24.2%
	max	48564	48898	49247	-	0.7% 1.4%
	average	5361	5677	6016	-	5.9% 12.2%
21-Dec	min	1763	1880	1966	-	6.6% 11.5%
	max	19906	19954	20006	-	0.2% 0.5%
	average	12340	12502	12682	-	1.3% 2.8%

The illuminance values frequency distributions over the work plan presented in Figure 9a,b clearly describe the effect of light distribution inside the room. In accordance with the specularity increase, the frequency distribution had a peak shift towards higher values of illuminance and a general redistribution that could be comparable to an increase in surface reflectance instead of the sole specularity.



(b)

Figure 9: Illuminance values frequency distribution, with a given specularity value of 0, 0.1 and 0.2. (a) Dec-21 (b) Jun-21

## Conclusion

This new approach for determining the interior surfaces' reflectance, and especially being thought for heterogeneous surfaces, has great potential to ease the material characterization and improve the accuracy of daylighting performance analysis in existing buildings. It also delivers a prompt response, without extensive and intensive laboratory tests compared to other alternative procedures. Moreover, this methodology can be applied to any kind of surface, that means that walls (including those with wall-papers or tapestry) and ceilings could be assessed with the same procedure, also surfaces that have an architectural value which can't be altered by any means. Nevertheless, further work is foreseen to improve the lighting exposition correction, and to provide flexibility for generating the boundary that isolates the reference sample (so far it can only be rectangular).

Although specularity might generate deviations, it won't be yet further assessed, as it will require a further study on how to obtain the images of the sample.

Given the ease of the use of the script and the versatility of its programming language, it is as well likely that it will be exploited for creating a Grasshopper component that is able to take 3 inputs (image, boundary coordinates and reference sample reflectance) and provide to the user the representative reflectance value for speeding any parametric analysis in existing buildings.

Furthermore, the preliminary simulations carried out shows that (with the assumed simulation model and hypothesis) gross assumptions can affect UDI (both increasing and decreasing) values up to 8% (relative, 4.2% absolute), CDA up to 0.54% and DA up to 1.00%.

## References

- ASTM international. (2012). E 903 Standard test method for solar absorptance reflectance and transmittance of materials using integrating spheres, *i*, 1–18.
- Bremilla, E., Hopfe, C. J., & Mardaljevic, J. (2018). Influence of input reflectance values on climate-based daylight metrics using sensitivity analysis. *Journal of Building Performance Simulation*, 11(3), 333–349. Retrieved from <https://doi.org/10.1080/19401493.2017.1364786>
- British Standard Institution (BSI). (1985). BS 8206-1 - Lighting for buildings — Part 1: Code of practice for artificial lighting.
- British Standard Institution (BSI). (2008). BS 8206-2 - Lighting for buildings – Part 2: code of practice for daylighting. *B.S. Institution*, 8206-2.
- British Standard Institution (BSI). (2010). BS 8493 - Light Reflectance Value ( LRV ) of a surface – Method of test, 22.
- British Standard Institution (BSI). (2011a). BS 4800 - Schedule of paint colours for building purposes.
- British Standard Institution (BSI). (2011b). BS EN ISO 11664-2: Colorimetry - Part 2 : CIE standard illuminants, 3.
- Cai, W., Yue, J., Dai, Q., Hao, L., Lin, Y., Shi, W., Huang, Y., et al. (2018). The impact of room surface reflectance on corneal illuminance and rule-of-thumb equations for circadian lighting design. *Building and Environment*, 141(April), 288–297. Elsevier. Retrieved from <http://linkinghub.elsevier.com/retrieve/pii/S0360132318303226>
- CIBSE. 2015. “AM11: Building Performance Modelling.” London.
- CIBSE/SLL. 2005. “Lighting Guide 7: Office Lighting.” London.
- CIBSE/SLL. 2011. “Lighting Guide 5: Lighting for Education.”
- European committee for standardization. (2011). BS EN 12464-1 - Light and lighting — Lighting of work places Part 1 : Indoor work places, 1–57.
- International Organization for Standardization. (2003). *ISO 9050: Glass in building — Determination of light transmittance, solar direct transmittance, total solar energy transmittance, ultraviolet transmittance and related glazing factors. Iso*.
- Illuminating Engineering Society. 2012. IES LM-83-12. Approved Method: IES Spatial Daylight Autonomy (sDA) and Annual Sunlight Exposure (ASE). New York: Illuminating Engineering Society
- Mardaljevic, J., Bremilla, E., & Drosou, N. (2015). Illuminance-Proxy High Dynamic Range Imaging : a Simple Method To Measure Surface Reflectance. *Proceedings of 28th International Commission on Illumination (CIE) Session 2015*, 363–372.
- Reinhart, C. F. (2002). Effects of Interior Design on the Daylight Availability in Open Plan Offices Daylighting in open plan offices. *Conference Proceedings of the ACEEE Summer Study on Energy Efficient Buildings*, 1(613), 1–12.
- Samant, S., & Yang, F. (2007). Daylighting in atria: The effect of atrium geometry and reflectance distribution. *Lighting Research & Technology*, 39(2), 147–157. Retrieved from <https://doi.org/10.1177/1365782806074482>
- Ward, G. and Shakespeare, R. (1998). *Rendering with Radiance: The Art and Science of Lighting Visualization*. Morgan Kaufman.
- Warrier, G. A., & Raphael, B. (2017). Performance evaluation of light shelves. *Energy and Buildings*, 140, 19–27. Retrieved May 23, 2017, from <http://www.sciencedirect.com/science/article/pii/S03787781730258X>
- Wienold, J., & Christoffersen, J. (2006). Evaluation methods and development of a new glare prediction model for daylight environments with the use of CCD cameras. *Energy and Buildings*, 38(7), 743–757.
- De Wilde, P. (2014). The gap between predicted and measured energy performance of buildings: A framework for investigation. *Automation in Construction*, 41, 40–49.
- Wolisz, H., Kull, T. M., Streblow, R., & Müller, D. (2015). The Effect of Furniture and Floor Covering Upon Dynamic Thermal Building Simulations. *Energy Procedia*, 78, 2154–2159. Retrieved from <https://linkinghub.elsevier.com/retrieve/pii/S1876610215020366>